Restoration of Potent Protein−Tyrosine Phosphatase Activity into the Membrane-Distal Domain of Receptor Protein−Tyrosine Phosphatase α†

Arjan Buist,‡ Yan-Ling Zhang,§ Yen-Fang Keng,§ Li Wu,§ Zhong-Yin Zhang,*,§ and Jeroen den Hertog*,‡

Hubrecht Laboratory, Netherlands Institute for Developmental Biology, Utrecht, The Netherlands, and Department of Molecular Pharmacology, Albert Einstein College of Medicine, Bronx, New York 10461

Received August 11, 1998; Revised Manuscript Received November 2, 1998

ABSTRACT: Most transmembrane, receptor-like protein−tyrosine phosphatases (RPTPs) contain two cytoplasmic catalytic protein−tyrosine phosphatase (PTP) domains, of which the membrane-proximal domain, D1, contains the majority of the activity, while the membrane-distal domain, D2, exhibits little or no activity. We have investigated the structural basis for reduced activity in RPTP-D2s, using RPTPα as a model system. Sequence alignment of PTP domains indicated that two motifs, the KNRY motif and the WpD motif, are highly conserved in all PTP domains, but not in RPTP-D2s. In RPTPα-D2, the Tyr in the KNRY motif is substituted by Val (position 555) and the Asp in the WpD motif by Glu (position 690). Mutation of Val555 and Glu690 had synergistic effects on RPTPα-D2 activity, in that the PTP activity of RPTPα-D2-V555Y/E690D was greatly enhanced to levels that were similar to or approaching those of RPTPα-D1. Therefore, Val555 and Glu690 are responsible in large part for reduced RPTPα-D2 activity. In addition, we established that the increased PTP activity is due to restoration of effective transition-state stabilization in RPTPα-D2-V555Y/E690D. Since the KNRY motif and the WpD motif are mutated in all RPTP-D2s, it is highly unlikely, due to lack of transition-state stabilization, that the residual RPTP-D2 catalytic activity plays a role in the function of RPTPs.

Protein−tyrosine phosphorylation is one of the major mechanisms controlling cell proliferation and differentiation. Protein−tyrosine phosphatases (PTPs)[1] catalyze the hydrolysis of phosphoryl groups on tyrosine residues in proteins and, together with protein−tyrosine kinases, regulate phosphotyrosine levels of cellular proteins. The family of PTPs is estimated to contain around 500 members of which more than 75 have been identified (*1*). The catalytic domain consists of about 240 amino acids and contains the active site sequence [I/V]HCxAGxxR[S/T]G, called the PTP signature motif, that defines the PTP family (*1*−*4*). The Cys within this sequence is absolutely essential for PTP activity, since it forms a Cys−phosphate intermediate during catalysis (*5*, *6*). The PTP domains are conserved not only in sequence but also in structure. Comparison of the crystal structures of PTP domains that have been solved thus far indicates that the overall folds of PTP1B, Yop51, RPTPα, RPTPμ, and SHP-2 are very similar (*7*−*11*).

The PTP family can be divided into two major groups: receptor-like and intracellular PTPs. Receptor-like PTPs (RPTPs), with CD45 as the founding member (*12*), consist of an extracellular domain, a single membrane spanning region, and one or, more commonly, two cytoplasmic PTP domains. The membrane-proximal PTP domain, D1, is catalytically active whereas the membrane-distal domain, D2, contains very little or no catalytic activity. In addition, it has been demonstrated that catalytic activity of D1, but not D2, is essential for the function of several RPTPs, including RPTPα, CD45, and CLR-1, in that inactivation of D1 is sufficient to abolish the biological activity of these RPTPs (*13*−*15*).

The function of D2s in RPTPs is not clear. The strongest suggestion for intrinsic phosphatase activity in D2 comes from work on RPTPα. Wang and Pallen (*16*) demonstrated that D2 of RPTPα has intrinsic activity when expressed in the absence of D1. By using *p*-nitrophenyl phosphate as a substrate, we showed the k_{cat} value for D2 to be only 10-fold lower than that of D1 with a 5-fold higher K_m (*17*). However, the activity of D2 toward pTyr-containing peptides was shown to be 5 orders of magnitude lower than D1 (*17*). For many other PTPs, D2 is unlikely to be catalytically active. D2s of HPTPγ and HPTPζ lack the catalytic site Cys within the signature motif (*18*, *19*), and most D2s lack the essential aspartic general acid/base. Mutation of the catalytic site Cys in D1 of CD45, LAR, or RPTPμ abolishes almost all the PTP activity while the same substitution in D2 has

† This work was supported by a grant from the Life Science Foundation/Netherlands Organization for Scientific Research (SLW/NWO) (to A.B.), a National Institutes of Health Grant CA69202 (to Z.-Y. Z.), Z.-Y. Z. is a Sinsheimer Scholar, and a grant from the Dutch Cancer Society (to J.d.H.).

* To whom correspondence should be addressed. J.d.H.: Hubrecht Laboratory, Netherlands Institute for Developmental Biology, Uppsalalaan 8, 3584 CT Utrecht, The Netherlands. Tel: +31-30-2510211. Fax: +31-30-2516464. E-mail: hertog@niob.knaw.nl. Z.-Y.Z.: Department of Molecular Pharmacology, Albert Einstein College of Medicine, 1300 Morris Park Avenue, Bronx, NY 10461. Tel: (718) 430 4288. Fax: (718) 430 8922. E-mail: zyzhang@aecom.yu.edu.

‡ Netherlands Institute for Developmental Biology.

§ Albert Einstein College of Medicine.

[1] Abbreviations: PTP, protein−tyrosine phosphatase; RPTP, receptor-like PTP; D1, membrane-proximal PTP domain; D2, membrane-distal PTP domain; *p*NPP, *para*-nitrophenyl phosphate; OMFP, 3-*O*-methylfluorescein phosphate; EGFR, epidermal growth factor receptor; PDGFR, platelet-derived growth factor receptor.

10.1021/bi981936b CCC: $18.00
Published on Web 12/23/1998

little or no effect on the PTP activity (*20*−*22*). In addition, recombinant D2 of LAR and CD45 by itself showed no detectable activity (*21*, *23*). Comparison of PTP domains from different RPTPs showed that in general D2s are more closely related to one another than to the D1 within the same PTP (*24*), suggesting that, even though D2s are not catalytically active, D2s are conserved and may have an important function.

To gain more insight into the function of the membrane-distal PTP domain of RPTPα, we compared the sequences of many PTP domains. Tyr262, located in the catalytic pocket of RPTPα-D1 (*9*), was almost absolutely conserved in RPTP-D1s and cytoplasmic PTPs, but not in D2s. In addition, the general acid/base Asp residue that is involved in catalysis is mutated in all D2s. We have investigated the effect of substitution of the corresponding residues, Val555 with Tyr and Glu690 with Asp, on the catalytic activity of D2 and found that these conserved residues are involved in transition-state stabilization. Moreover, we demonstrate that reversing Val555 to Tyr together with Glu690 to Asp converted this domain into a very potent PTP domain with enzymatic characteristics that are comparable to RPTPα-D1, suggesting that Val555 and Glu690 are responsible for the reduced PTP activity of RPTPα-D2.

MATERIALS AND METHODS

Materials. *p*-Nitrophenyl phosphate (*p*NPP), β-naphthyl phosphate, glutathione-agarose beads, and human thrombin were purchased from Sigma. Phosphotyrosine (pTyr)-containing peptides DTSSVLpYTAVQ ($PDGFR^{1003-1013}$), EGDNDpYIIPL ($PDGFR^{1016-1025}$), and Ac-DAFSDpYANFK ($PTP\alpha^{784-793}$) were prepared by the Laboratory of Macromolecular Analysis of the Albert Einstein College of Medicine. The pTyr-containing peptide DADEpYLIPQQG ($EGFR^{988-998}$) was synthesized, purified, and characterized as described previously (*25*). Vanadium (V) oxide (99.99%) was obtained from Aldrich. Solutions were prepared using deionized and distilled water.

Constructs and Mutagenesis. Expression vectors for bacterial expression of RPTPα glutathione *S*-transferase fusion proteins were derived by insertion of polymerase chain reaction-generated *Nco*I-*Hin*dIII fragments into pGEX-KG opened with *Nco*I and *Hin*dIII (26). The bacterial expression vector encoding the complete cytoplasmic region of RPTPα (residues 167−793; numbering according to ref *27*) has been described (*28*). The expression vectors for RPTPα-D1 (residues 167−503) and RPTPα-D2 (residues 504−793) were derived using the oligonucleotide pairs NI, CII and NIV, CI respectively: NI, 5′-GCGCCATGGCGAAGAAATACAAGCA; CII, 5′-CCCTCAAGCTTCCAGTTCTGTGTCCCCATA; NIV, 5′-CCCATGGCTTCTCTAGAAACC; and CI, 5′-CGCAAGCTTTCACTTGAAGTTGGC. Site-directed mutagenesis was done on the full-length RPTPα cDNA in pSG5, pSG-RPTPα (*13*). Mutations were verified by sequencing, and subsequently, the corresponding glutathione *S*-transferase fusion protein expression vectors were constructed as described above. The oligonucleotides that were used for site-directed mutagenesis are the following: RPTPα-D1-Y262V, 5′-AAAAACCGCGTTGTAAACATC; RPTPα-D2-V555Y, 5′-AAGAACCGGTATTTACAGATC; and RPTPα-D2-E690D, 5′-GGCTGGCCTGATGTGGGCATC.

Recombinant Enzymes. The RPTPα−glutathione *S*-transferase fusion protein constructs were transformed into *Escherichia coli* BL21(DE3). Overnight cultures of BL21-(DE3) cells containing pGEX recombinant plasmids for RPTPα were diluted 100-fold and grown at 37 °C until the absorbance at 600 nm reached 0.6. Expression of glutathione *S*-transferase fusion proteins was then induced by isopropyl-1-thio-β-D-galactopyranoside (100 μM, final concentration), overnight at room temperature. Purification of the RPTPα−glutathione S-transferease fusion proteins by glutathione agarose beads and the subsequent thrombin cleavage of the glutathione *S*-transferase fusion protein was done exactly as described (*26*). The recombinant RPTPα proteins were at least 90% pure as judged by SDS−PAGE electrophoresis and coomassie staining of the gels.

PTP assays and Determination of Kinetic Constants Using Various Substrates. The PTP activity with *p*NPP as a substrate was assayed at 30 °C in a 200 μl reaction mixture. The reaction mixture contained the appropriate concentration of *p*NPP, 50 mM succinate, pH 6.0, and 1 mM EDTA, and the ionic strength of the solutions was kept at 0.15 M using NaCl. The reaction was initiated by the addition of enzyme and quenched after 4 min by the addition of 1 mL of 1 N NaOH. The nonenzymatic hydrolysis of the substrate was corrected by measuring the control without the addition of enzyme. The amount of product *p*-nitrophenol was determined from the absorbance at 405 nm using a molar extinction coefficient of 18 000 M^{-1} cm^{-1}. The kinetic constants for the PTP-catalyzed hydrolysis of β-naphthyl phosphate and pTyr-containing peptide substrates were determined by following the production of inorganic phosphate (25). k_{cat} and K_m values were calculated from a direct fit of the v versus [S] data to the Michaelis−Menten equation using a direct curve-fitting program KINETASYST (IntelliKinetics, State College, PA). The kinetic constants for the PTP-catalyzed hydrolysis of pTyr-containing peptide substrates were also determined by continuously monitoring at 305 nm for the increase in tyrosine fluorescence with excitation at 280 nm (*25*). The data were analyzed using a nonlinear least-squares regression program (KaleidaGraph, Synergy Software). When $[S] \ll K_m$ the reaction is first-order with respect to [S]. At a given enzyme concentration, the observed apparent first-order rate constant is equal to $(k_{cat}/K_m)[E]$. The substrate specificity constant k_{cat}/K_m value is calculated by dividing the apparent first-order rate constant by the enzyme concentration. Fluorimetric determinations were performed on a Perkin-Elmer LS50B fluorimeter. The instrument was equipped with a water-jacketed cell holder, permitting maintenance of the reaction mixture at the desired temperature (30 °C). Both methods yielded similar results.

Pre-Steady-State Kinetics. Pre-steady-state kinetic measurements of D1-, D2-, D2-V555Y-, D2-E690D-, and D2-V555Y/E690D-catalyzed hydrolysis of *p*NPP and 3-*O*-methylfluorescein phosphate (OMFP) were carried out at pH 6.0 and 25 °C using an Applied Photophysics MX.17MV sequential stopped-flow spectrophotometer. The reaction was monitored by the increase in absorbance at 430 nm for *p*-nitrophenolate (extinction coefficient 740 M^{-1} cm^{-1}) or 477 nm for 3-*O*-methylfluorescein (OMF) (extinction coefficient 25 000 M^{-1} cm^{-1}), respectively. The enzyme concentration after mixing was 30 μM for D1, 50 μM for D2, D2-E690D, and D2-V555Y/E690D, and 40 μM for D2-

V555Y, respectively. The concentrations for *p*NPP and OMFP were 200 and 2 mM, respectively, after mixing. OMFP was prepared in 50 mM succinate, 1 mM EDTA, pH 6.0, buffer containing 20% DMSO. Data analysis was performed as previously described (*43*).

Determination of Inhibition Constants. The stock solution of sodium orthovanadate was prepared as described (*17*). Briefly, vanadium (V) oxide was dissolved in 1 molar equiv/vanadium atom of 1.0 M aqueous NaOH. The resulting orange solution (mainly decavanadate) was boiled, allowed to stand overnight, and pH adjusted to 10. The final solution was colorless containing mainly orthovanadate (*29*). The inhibition constants for arsenate, vanadate, and β-naphthyl phosphate were determined for the PTPs as follows: the initial rate at various *p*NPP concentrations was measured following the production of *p*-nitrophenol (*30*). All inhibition experiments with vanadate were performed in the absence of EDTA since EDTA forms a very stable 1:1 complex with vanadate (*31*). The inhibition constant and inhibition pattern were evaluated using a direct curve-fitting program KINETASYST (IntelleKinetics, State College, PA).

RESULTS

Lack of Conservation of KNRY and WpD Motifs in RPTP-D2s. To investigate the basis for the relatively low activity of RPTPα-D2, we compared RPTPα-D1 and -D2 with a selection of PTP domains of human RPTPs of each subclass (*32*) and intracellular PTPs. There are two highly conserved motifs in PTP domains with demonstrable activity that are not conserved in D2s: the KNRY motif, which is located in the N-terminal region of the PTP domains (Figure 1A), and the WpD motif (Figure 1B), which contains the Asp residue that acts as a general acid/base in catalysis (*33*, *34*). The Tyr within the KNRY motif is conserved in most PTP domains, but not in D2s. In PTP1B, Tyr46 in the KNRY motif has been shown to be located in the catalytic pocket near the aromatic ring of the pTyr of cocrystallized pTyr-containing peptides, suggesting a role in substrate binding (*35*). From the crystal structure of RPTPα-D1 it is clear that this Tyr residue is also located in the catalytic pocket of this domain (*9*). Although the overall 3-D structure of RPTPα-D2 is very similar to that of other PTPs, the conserved Tyr of the KNRY motif is missing from the catalytic site pocket of RPTPα-D2.[2]

The WpD motif (for the conserved Trp-Pro-Asp) resides in a surface loop that alternates between an open and a closed form (*35*, *36*). After substrate binding the closed conformation of the flexible WpD loop is stabilized by the bound substrate so that the Asp is close enough to the scissile oxygen of the substrate for catalysis (*35*, *36*). The essential Asp is highly conserved among RPTP-D1s and the catalytic domains of intracellular PTPs, but is mutated in all known RPTP-D2s. In RPTPα-D2 the corresponding Asp in the WpD motif is replaced by a Glu (Figure 1B). Previously, we have demonstrated that reverting this residue into an Asp modestly increases the activity of D2 (*17*). Therefore, the absence of the Asp in the WpD motif is not the only cause for the relatively low PTP activity of RPTPα-D2. The RPTP IA-2 contains only a single PTP domain that lacks the Asp in the WpD motif (Ala), as well as the Tyr in the KNRY motif (His) (*37*, *38*). Interestingly, IA-2 does not display detectable PTP activity (*37*).

The PTP signature motif [I/V]HCxAGxxR[S/T]G containing the Cys residue that is essential for catalysis is highly conserved in all PTP domains (Figure 1C). The essential Cys is conserved in all D1s and in the PTP domains of the intracellular PTPs. In RPTPγ-D2 the Cys is replaced by an Asp, suggesting that RPTPγ-D2 is inactive. In RPTPα, the essential Cys in the signature motif in D2 is conserved. Other residues in the signature motif that have been shown to be essential for catalysis (*21*, *39*) are also conserved in RPTPα-D2. Therefore, the relatively low activity of RPTPα-D2 is not due to alterations in the signature motif. Taken together, there are only two general differences between D1s and cytoplasmic PTPs on one hand and D2s on the other. The Tyr in the KNRY motif is never present in D2s, while it is highly conserved in other PTP domains, and the general acid/base Asp residue in the WpD motif, which is invariant in RPTP-D1s and cytoplasmic PTPs, is not conserved in RPTP-D2s.

The KNRY and WpD Motifs are Important for Catalysis. To investigate whether mutations in the KNRY motif (Val555 instead of Tyr) and WpD motif (Glu690 instead of Asp) account for the low PTP activity in D2, we converted RPTPα Val555 to Tyr and Glu690 to Asp. First we determined the steady-state kinetic parameters of wild-type RPTPα-D1 and -D2 using *p*NPP as the substrate (Table 1A). As shown before (*17*), the k_{cat} of D2 was 10-fold lower than that of D1 while the K_m was 5-fold higher. Mutation of Val555 to Tyr (D2-V555Y) did not alter the k_{cat}, but lowered the K_m by 5-fold. As a control we converted the situation in D1 to that of D2 by mutating the Tyr in the KNRY motif to a Val. TheY262V mutation increased the K_m of D1 by almost 8-fold and lowered the k_{cat} by more than 5-fold. Mutation of the general acid/base Asp401 in the WpD motif in D1 abolished almost all PTP activity (17). Substitution of Glu690 in D2 to Asp increased k_{cat} by 3.5-fold but also increased K_m 2-fold (Table 1A; ref *17*). Interestingly, RPTPα-D2 containing both the Val555 to Tyr and Glu690 to Asp substitutions (D2-V555Y/E690D) showed a 12-fold increase in k_{cat} and a 3-fold decrease in K_m, resulting in a 34-fold increase in the substrate specificity constant, k_{cat}/K_m, which was in the same range as the k_{cat}/K_m of D1 (Table 1A).

The pK_a of the leaving group in *p*NPP is relatively low (pK_a = 7.14) compared to pTyr-containing substrates (pK_a = 10.07). A leaving group with a higher pK_a is more difficult to expel because of the negative charge that develops on the phenolate oxygen in the transition state (*40*). Thus, *p*NPP has a much higher intrinsic chemical reactivity than pTyr. To show that the enhanced phosphatase activity is due to improvements in D2 itself, we also determined the steady-state kinetic parameters of the different mutants using a substrate with a higher pK_a, β-naphthyl phosphate (pK_a = 9.38) (Table 1B). Like for *p*NPP, mutating Val555 to Tyr or Glu690 to Asp had only minor effects on k_{cat} and K_m of D2 with β-naphthyl phosphate as the substrate. However, the k_{cat} of the D2-V555Y/E690D double mutant was 15-fold higher with a small decrease in K_m. The k_{cat}/K_m value for D2-V555Y/E690D was more than 2-fold higher than that for D1, indicating that the substrate specificity toward β-naphthyl phosphate of the D2 double mutant was even higher than D1. These results show that RPTPα-D2-V555Y/

[2] A. Bilwes and J. Noel, personal communication.

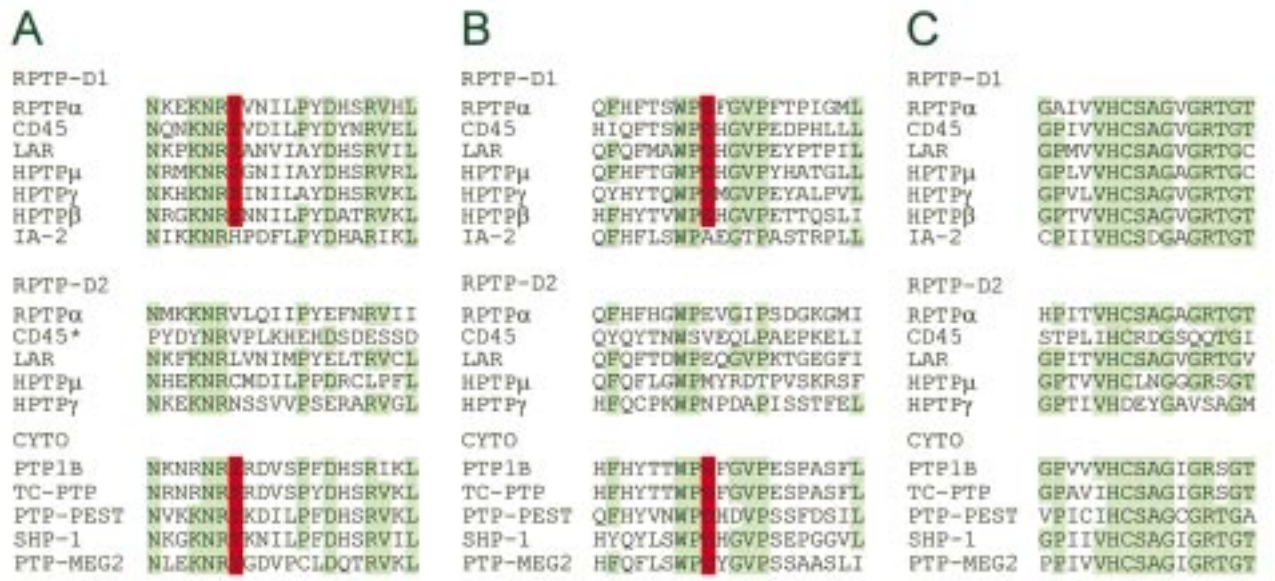

FIGURE 1: Conservation of the KNRY and WpD motifs. Sequence alignment of the PTP domains of mouse RPTPα (27), human CD45 (49), human LAR (50), HPTPμ (51), HPTPγ (18), HPTPβ (18), IA-2 (38), PTP1B (52), TC-PTP (53), PTP-PEST (54), SHP-1 (55), and PTP-MEG2 (56). RPTP-D1s and -D2s as well as the PTP domains of cytoplasmic PTPs (cyto) are depicted. The RPTPs HPTPβ and IA-2 contain a single PTP domain and are listed under the RPTP-D1s. (A) Alignment of the first 20 amino acids of the different PTP domains (residues 256−275 and 549−568 in RPTPα-D1 and -D2, respectively). For simplicity, an insertion of 8 residues was omitted in CD45-D2 (CD45*). The complete sequence of this segment is DYDYNRVPLKHELEMSKESEHDSDESSD. (B) Alignment of the amino acids surrounding the WpD motif (residues 393−412 and 682−701 in RPTPα-D1 and -D2, respectively). (C) The PTP signature motif (residues 427−442 and 717−732 in RPTPα-D1 and -D2, respectively). The Tyr in the KNRY motif and the Asp in the WpD motif that are conserved in all PTP domains of the cytoplasmic PTPs and RPTP-D1s but mutated in all RPTP-D2s are indicated in red, and other conserved residues are indicated in green.

Table 1: RPTPα-D2-V555Y/E690D is a Potent PTP[a]

	k_{cat} (s^{-1})	K_m (mM)	k_{cat}/K_m (s^{-1} mM^{-1})
A. *p*NPP			
RPTPα-D1	9.3 ± 0.6	3.9 ± 0.7	2.4 ± 0.5
RPTPα-D1-Y262V	1.7 ± 0.04	30 ± 3	0.057 ± 0.006
RPTPα-D2	0.98 ± 0.05	21 ± 0.7	0.047 ± 0.003
RPTPα-D2-V555Y	0.92 ± 0.03	4.0 ± 0.6	0.23 ± 0.04
RPTPα-D2-E690D	3.5 ± 0.2	39 ± 5	0.09 ± 0.01
RPTPα-D2-V555Y/E690D	12 ± 0.7	7.7 ± 1	1.6 ± 0.2
B. β-naphthyl phosphate			
RPTPα-D1	6.4 ± 0.2	7.3 ± 1	0.88 ± 0.1
RPTPα-D1-Y262V	0.41 ± 0.04	4.7 ± 1	0.087 ± 0.02
RPTPα-D2	0.48 ± 0.02	6.2 ± 0.7	0.077 ± 0.009
RPTPα-D2-V555Y	0.31 ± 0.01	2.9 ± 0.3	0.11 ± 0.01
RPTPα-D2-E690D	0.95 ± 0.05	6.0 ± 1	0.16 ± 0.03
RPTPα-D2-V555Y/E690D	7.6 ± 0.4	3.8 ± 0.5	2.0 ± 0.3

[a] Steady-state kinetic constants determined for various forms of RPTPα using *p*NPP (A) or β-naphthyl phosphate (B) as substrates. All assays were performed at pH 6.0 and 30 °C.

E690D is a very potent PTP. pTyr-containing peptides more closely resemble in vivo substrates than artificial substrates, like *p*NPP and β-naphthyl phosphate. Therefore, steady-state kinetic parameters were determined using pTyr-containing peptides corresponding to Tyr (auto)phosphorylation sites in the epidermal growth factor receptor (EGFR pY992), platelet-derived growth factor receptor (PDGFR pY1009 and pY1021), or RPTPα (pY789). The different mutants in D1 and D2 showed only a moderate selectivity toward the various substrates with a maximum of a 13-fold difference in k_{cat}/K_m among the peptides (Table 2). Like we have shown before, reverting Glu690 to Asp increased k_{cat}/K_m 4-fold (*17*). Reverting Val555 to Tyr increased k_{cat}/K_m 4−24-fold. However, the mutant containing both Val555 to Tyr and Glu690 to Asp mutations displayed a k_{cat}/K_m that is 130−300-fold higher than wild-type D2. For *p*NPP, the substrate specificity constant of D2-V555Y/E690D was similar to that of wild-type D1 (Table 1A). Using phosphopeptides the double mutant exhibited k_{cat}/K_m values that were only 40−200-fold lower than D1, indicating that RPTPα-D2-V555Y/E690D is a potent PTP.

Inhibition by Arsenate, Vanadate, and β-Naphthyl phosphate. To gain more insight into the role of the conserved KNRY and WpD motifs in catalysis, we determined inhibition constants of arsenate (a product analog), vanadate (a transition-state analog), and β-naphthyl phosphate (a substrate analog) for D1, D2, and the different mutants. The inhibition constants were determined using *p*NPP as a substrate. For both D1 and D2 arsenate was a weak competitive inhibitor with a K_i in the millimolar range, albeit arsenate inhibited RPTPα-D1 30-fold more strongly than D2. The different mutations had very little effect on the K_i of arsenate (Figure

Table 2: Summary of Kinetic Constants with pTyr-Containing Peptides as Substrates

substrate/enzyme	k_{cat} (s^{-1})	K_m (mM)	k_{cat}/K_m (M^{-1} s^{-1})
Ac-DAFSDpYANFK (PTPα$^{784-793}$)			
RPTPα-D1	9.7 ± 0.6	0.29 ± 0.04	(3.3 ± 0.5) × 10^4
RPTPα-D1-Y262V	0.0073 ± 0.0008	2.69 ± 0.62	2.7 ± 0.7
RPTPα-D2	0.025 ± 0.003	5.9 ± 0.9	4.2 ± 0.8
RPTPα-D2-V555Y	0.092 ± 0.006	0.89 ± 0.18	100 ± 22
RPTPα-D2-E690D	0.066 ± 0.006	5.5 ± 0.7	2 ± 2
RPTPα-D2-V555Y/E690D	1.5 ± 0.11	1.7 ± 0.2	880 ± 110
DTSSVLpYTAVQ (PDGFR$^{1003-1013}$)			
RPTPα-D1	26 ± 1	0.15 ± 0.02	(1.7 ± 0.2) × 10^5
RPTPα-D1-Y262V	0.044 ± 0.003	2.5 ± 0.37	18 ± 4
RPTPα-D2	0.011 ± 0.001	1.5 ± 0.3	7.3 ± 2
RPTPα-D2-V555Y	0.090 ± 0.005	1.4 ± 0.15	64 ± 8
RPTPα-D2-E690D	0.038 ± 0.002	1.4 ± 0.3	27 ± 6
RPTPα-D2-V555Y/E690D	1.3 ± 0.06	1.4 ± 0.13	930 ± 96
EGDNDpYIIPL (PDGFR$^{1016-1025}$)			
RPTPα-D1	14 ± 0.3	0.32 ± 0.01	(4.4 ± 0.04) × 10^4
RPTPα-D2	0.0074 ± 0.0005	3.0 ± 0.3	2.5 ± 0.3
RPTPα-D2-E690D	0.032 ± 0.016	3.2 ± 1.7	10 ± 7
RPTPα-D2-V555Y/E690D			744 ± 1
DADEpYLIPQQG (EGFR$^{988-998}$)			
RPTPα-D1	9.1 ± 0.3	0.060 ± 0.006	(1.5 ± 0.2) × 10^5
RPTPα-D1-Y262V			35 ± 0.1
RPTPα-D2	0.017 ± 0.02	4.5 ± 3.2	3.8 ± 4.2
RPTPα-D2-V555Y			17 ± 0.1
RPTPα-D2-V555Y/E690D			742 ± 27

2A). These results indicate that alterations in these residues do not lead to significant structural changes in the active sites of D1 or D2.

Vanadate is a far more potent inhibitor of PTPs and is thought to act as a transition-state analogue for the PTP-catalyzed reaction due to its tendency to adopt a pentavalent geometry. When bound in the PTP active site, the vanadium atom is within covalent bonding distance of the Sγ of the active site Cys residue and vanadate adopts a slightly distorted trigonal bipyramidal geometry (*41*, *42*) that resembles the transition state for the hydrolysis of the thiophosphate enzyme intermediate in the PTP-catalyzed reaction (*4*, *43*). In solution, vanadate inhibited the RPTPα-D1- and -D2-catalyzed reaction reversibly and competitively, with dissociation constants of 5.5 and 1900 μM, respectively (Figure 2B). Thus, the affinity of D1 for vanadate is 350-fold higher than that of D2. The D1-Y262V mutant was 7-fold less inhibited by vanadate than wild-type D1. Mutating Val555 to Tyr, however, decreased the K_i for D2 only by 3.5-fold. In addition, mutation of the Glu690 to Asp decreased the K_i of vanadate for D2 2-fold. Surprisingly, the affinity of D2-V555Y/E690D double mutant for vanadate increased 230-fold in comparison with D2 and was similar to that of D1 (Figure 2B).

Analysis of the ability of the low molecular weight aryl phosphate substrate, β-naphthyl phosphate, to serve as an inhibitor of the PTP-catalyzed hydrolysis of *p*NPP indicated that the inhibition pattern for β-naphthyl phosphate was competitive with respect to *p*NPP (data not shown). The apparent K_i values for β-naphthyl phosphate were similar for RPTPα-D1 and -D2. As is the case for arsenate inhibition, mutation of Tyr262 in D1 or Val555 and Glu690 in D2 only led to a modest change (3−8-fold) in the affinity for β-naphthyl phosphate (Figure 2C). These results demonstrate that inhibition by the substrate analogue β-naphthyl phosphate is not significantly different for RPTPα-D1 or -D2 or any of the mutants.

Taken together, these inhibition studies indicate that Tyr555 and Asp690 in D2-V555Y/E690D are important for transition-state stabilization. One of the major means an enzyme utilizes to catalyze a reaction is via transition-state stabilization. Since RPTPα-D1 stabilizes the transition state much better than D2 it is clear that RPTPα-D1 is a better PTP than D2. Reverting both Val555 to Tyr and Glu 690 to Asp restores the transition-state-stabilizing ability of D2 and converts D2 into a very potent PTP.

Pre-Steady-State Kinetics. PTP-catalyzed reactions utilize a double-displacement mechanism in which the side chain of the active site Cys residue serves as a nucleophile to accept the phosphoryl group from the substrate and form a kinetically competent cysteinyl phosphate intermediate. The phosphoenzyme intermediate is subsequently hydrolyzed by water. Pre-steady-state stopped-flow experiments were performed in order to determine the rate-limiting step and the effects of mutation in D2 on the individual steps of the reaction. We initially used *p*NPP as a substrate which upon the action of the PTP should produce a "burst" of *p*-nitrophenolate if the net rate of phosphoenzyme intermediate is slower than that of intermediate formation. Unfortunately, the K_m values of *p*NPP for the various D1 and D2 PTPs ranged from 4 to 40 mM. To saturate the enzyme, one would have to use a very high concentration of *p*NPP. Since *p*NPP itself also absorbs at 405 nm, the background due to the presence of high substrate concentration was so enormous that the observation of a meaningful burst was technically difficult. We then tested 3-*O*-methylfluorescein phosphate (OMFP) as a substrate. The K_m values for OMFP were 1−4 mM for D2 and its mutants. The reaction was monitored by the increase in absorbance at 477 nm for 3-*O*-methylfluorescein (extinction coefficient 25 000 M^{-1} cm^{-1}). Although significant burst traces were observed for D2, D2-V555Y, D2-E690D, and possibly D2-V555Y/E690D at 2 mM OMFP concentration (data not shown), the data did not allow an unambiguous determination of the rates for the individual steps because it was impossible to obtain saturable concentrations of OMFP under our experimental conditions. The highest attainable OMFP concentration at pH 6 in 20%

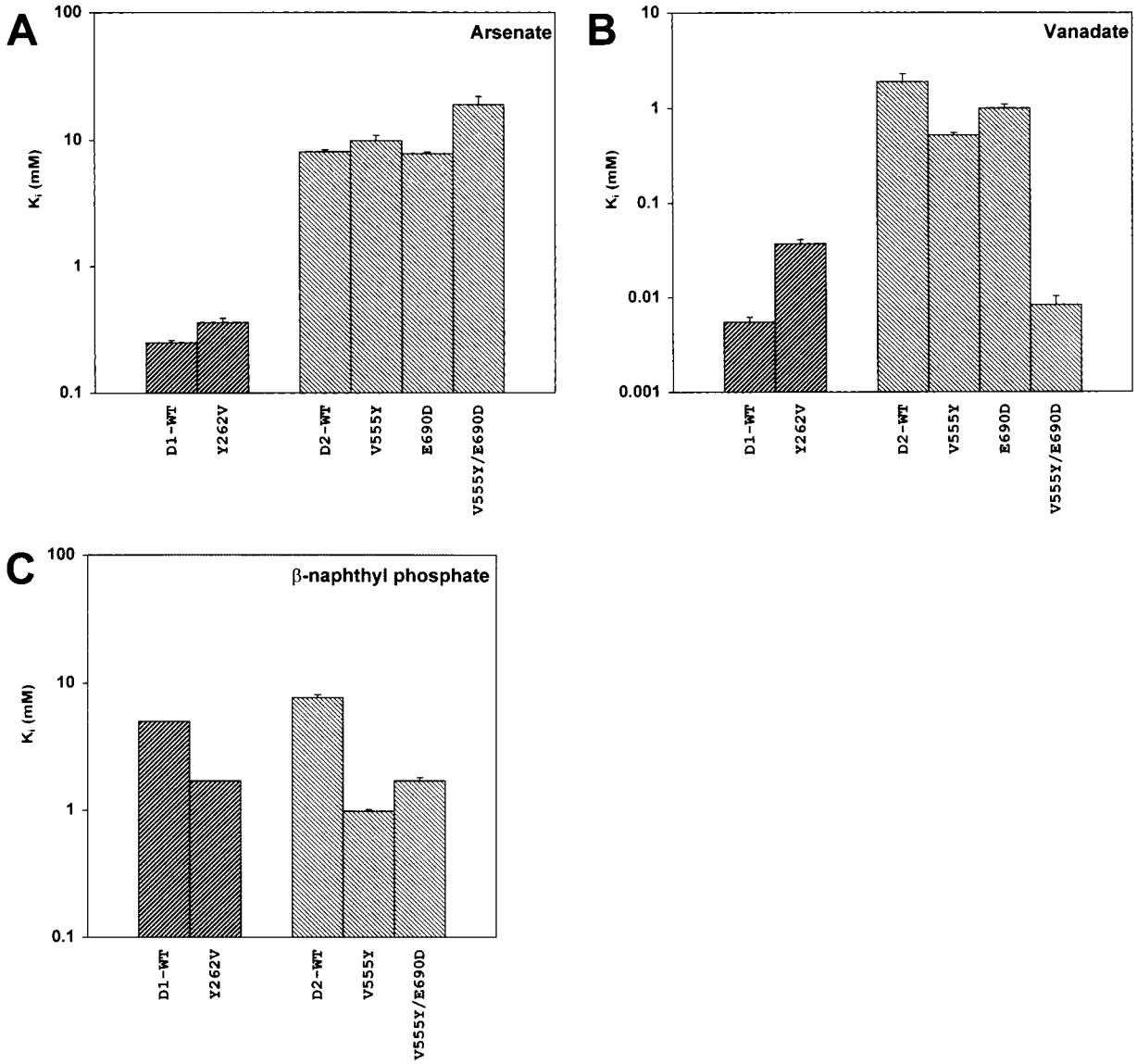

FIGURE 2: Inhibition by arsenate, vanadate, and β-naphthyl phosphate. The inhibition constants, K_i, were determined for arsenate (A), vanadate (B), and β-naphthyl phosphate (C) using RPTPα-D1 or -D2 and mutants as indicated. All assays were performed at pH 6.0 and 30 °C, using *p*NPP as the substrate.

DMSO was 4 mM which, upon mixing with an equal volume of enzyme, gave a final concentration of 2 mM. Nevertheless, it appears that both chemical steps contribute to the rate-limiting reaction and the Val555 and Glu690 substitutions increase the rates of both chemical steps.

DISCUSSION

Most RPTPs contain two PTP domains, of which D1 exhibits PTP activity, while D2 contains little or no PTP activity. The structures of the catalytic domains of the cytoplasmic PTPs and the D1s of receptor-like PTPs that have been solved indicate that the overall folds and the configuration of the active sites are very similar to one another (*7*−*11*). In addition, the overall structure and active site configuration of RPTPα-D2 are similar to the known PTP domains,[2] indicating that there are no major differences in structure that may account for the difference in catalytic activity between RPTPα-D1 and -D2. Sequence alignment of many PTP domains revealed two highly conserved motifs, KNRY and WpD, in PTP domains with demonstrable activity that are not conserved in D2s.

The WpD motif is a flexible loop that contains the Asp residue that acts as a general acid/base in catalysis. This essential Asp is highly conserved among RPTP-D1s and the catalytic domains of intracellular PTPs, but is mutated in all known RPTP-D2s. Mutation of the Asp in WpD motifs of active PTPs reduces the turnover number by over 3 orders of magnitude (*17*, *33*). Since the general acid/base Asp is not conserved in D2s, this is a good candidate residue to be responsible for the reduced activity in D2s.

The KNRY motif is located in the N-terminal region of PTP domains and is involved in interactions with the substrate. The Tyr within the KNRY motif is conserved in most PTP domains, but not in D2s. In the structure of PTP1B complexed with a pTyr-containing peptide, the side chain of Tyr46 (corresponding to Tyr262 in RPTPα) forms interactions with the main-chain atoms and the aromatic ring of pTyr (*35*). Substitution of the Tyr side chain by a methyl group at position 46 in PTP1B (Y46A) resulted in a 7-fold decrease in k_{cat} and a 9-fold increase in K_m with *p*NPP as a substrate (*44*). In addition, mutating Tyr46 to Ser or Leu in

PTP1B led to a 15-fold decrease in k_{cat} and a 17-fold increase in K_m using tyrosine phosphorylated lysozyme as a substrate (*45*). Together, these data suggest that the lack of conservation of this Tyr in D2s may also partially account for the lack of activity in D2s.

We have previously shown that converting Glu690 in D2 back to Asp increases the activity of D2 by only 4-fold (*17*). We have therefore focused our effort on the Tyr residue. To establish the importance of Tyr262 in D1 catalysis, we replaced it with a Val residue which occupies the corresponding position in D2. As shown in Table 1, RPTPα-D1-Y262V displayed a 5.5- and 42-fold reduction in k_{cat} and k_{cat}/K_m, respectively, with *p*NPP as a substrate. When pTyr-containing peptides were used as substrates, the k_{cat} and k_{cat}/K_m for RPTPα-D1-Y262V were 10^3- and 10^4-fold lower than those of the wild-type D1 (Table 2). Thus, consistent with results obtained with PTP1B, the aromaticity of Tyr262, not the hydrophobicity, is important for D1 catalysis. We next substituted the corresponding Val555 in D2 by a Tyr residue. Surprisingly, this mutation in D2 did not have any effect on k_{cat} for the hydrolysis of *p*NPP but did improve the k_{cat}/K_m by 5-fold. In addition, RPTPα-D2-V555Y exhibited only a 4−8-fold increase in k_{cat} and a 4−24-fold increase in k_{cat}/K_m toward phosphopeptide substrates, in comparison with native D2.

Interestingly, when we mutated both Val555 and Glu690 in RPTPα-D2 into the corresponding Tyr and Asp in RPTPα-D1, the resulting RPTPα-D2-V555Y/E690D became a potent PTP (Tables 1 and 2). In fact, the catalytic activity of the double mutant for *p*NPP was similar to that of wild-type D1, and its activity for β-naphthyl phosphate was slightly higher than that of D1. For peptide substrates, the k_{cat} and k_{cat}/K_m for RPTPα-D2-V555Y/E690D were 60−120- and 130−300-fold higher than those for the native D2 domain, respectively. Thus, structure-based substitutions at positions 555 and 690 in D2 appear to have synergistic effects. The k_{cat}/K_m values for the RPTPα-D2-catalyzed dephosphorylation of pTyr-containing peptides are 10^5-fold lower than for D1 (*17*). Amazingly, k_{cat}/K_m values for the RPTPα-D2-V555Y/E690D-catalyzed dephosphorylation of pTyr peptides were only 40−200-fold lower than for D1. In fact, the activity of RPTPα-D2-V555Y/E690D is higher than some PTPs and most of the dual specificity phosphatases.

To gain more insight into the structural and chemical basis for the increased activity of the RPTPα-V555Y/E690D mutant, we performed inhibition studies. It is important to differentiate ground-state effects from transition-state effects. The affinities of D2-V555Y/E690D for β-naphthyl phosphate (a substrate analog) and arsenate (a product analog) were not significantly different from native RPTPα-D2 (Figure 2). In contrast, the wild-type D2 was inhibited by vanadate in the millimolar range, suggesting a very weak interaction, whereas RPTPα-V555Y/E690D was inhibited by vanadate in the micromolar range. Since vanadate has been shown to be a transition-state analogue, it is clear that the transition state in the wild-type D2-catalyzed reaction is not very well-stabilized. Accordingly, the chemical basis for the increased PTP activity in D2-V555Y/E690D is likely due to enhanced transition-state stabilization corroborated by both the KNRY and WpD motifs.

The structural basis for the enhanced transition-state binding by D2-V555Y, D2-E690D, and D2-V555Y/E690D is suggested by the following. In the structure of the PTP1B−vanadate complex, the apical oxygen atom, which resembles the leaving group oxygen or the oxygen atom of the attacking nucleophilic water molecule, forms a hydrogen bond with the carboxylate group of the Asp general acid/base (*42*). This is consistent with the Asp residue playing a role in stabilizing the transition state. Although the Tyr residue in the KNRY motif does not interact directly with vanadate, its presence in the active site may be important for the precise geometric alignment of residues involved in transition-state stabilization. Indeed, the OH group of Tyr46 in PTP1B forms a hydrogen bond with the side chain of Ser216 (*35*). Ser216 is part of the PTP signature motif which binds the terminal phosphate (or vanadate) oxygens with the main-chain NH groups. Computer simulations indicate that on average these NH groups form stronger hydrogen bonds with the terminal oxygens in the transition-state than in the ground state (*46*). The conserved Tyr residue in the KNRY motif may help to position the phosphate-binding loop for effective transition-state stabilization. Thus, it is understandable that both Asp690 and Tyr555 contribute to transition-state stabilization. In the D2 domains, the corresponding Tyr and Asp residues are replaced by Val and Glu, respectively, which would weaken the interactions between the PTP active site and the transition-state, resulting in a reduced PTP activity.

It is interesting to note that the D2-V555Y/E690D double mutant restored more than the added activity gains of the two single mutants D2-V555Y and D2-E690D. Since it was not possible to determine the specific contribution from each of the chemical steps to the k_{cat} parameter, we have restricted our discussion to the kinetic parameter k_{cat}/K_m, which is composed of rate constants for steps leading to the formation of the phosphoenzyme intermediate. Given the small magnitudes of k_{cat}/K_m for D2 and its mutants, it is likely that k_{cat}/K_m is controlled by chemistry, that is, phosphoenzyme formation (*40*). As shown in Tables 1 and 2, single conversion of Val555 to a Tyr in D2 resulted in a 5-fold increase in k_{cat}/K_m for *p*NPP and a 4−24-fold increase in k_{cat}/K_m for phosphopeptides. Similarly, single conversion of Glu690 to an Asp in D2 increased the k_{cat}/K_m by 2-fold for *p*NPP and 4-fold for phosphopeptides. However, the k_{cat}/K_m for the double mutant D2-V555Y/E690D was increased by 34- and 130−300-fold toward *p*NPP and phosphopeptides, respectively, suggesting that the two point mutations act synergistically to enhance the rate for phosphoenzyme formation. This is nicely supported by the vanadate-binding data (Figure 2) which paralleled the kinetic observations. Therefore, the restoration of PTP activity into D2 is primarily due to improved transition-state stabilization.

The potential outcomes of enzyme double mutations on catalysis and binding have been thoroughly discussed (*47*). Since the conserved Tyr in the KNRY motif and the conserved Asp in the WpD motif do not interact directly with each other, the observed synergistic effects on k_{cat}/K_m are most likely due to the simultaneous action of both residues on the same chemical step, which, together, have a greater total effect than the sum of their individual effects. Thus, on the basis of the preceding discussion, the conserved Tyr functions to orient the phenyl ring of the substrate and to stabilize the phosphate-binding loop for effective transition-state binding. Furthermore, these interactions should also help to fix the substrate in the optimal position thereby

facilitating the protonation of the leaving group oxygen by the conserved Asp. Conversely, the interaction between the Asp with the leaving group oxygen in the transition state should also lead to synergistic enhancement in the interactions between the conserved Tyr and the transition state. The fact that the k_{cat}/K_m values for D2-V555Y/E690D double mutant with peptide substrates are still lower than those of D1 suggests that differences between D1 and D2 outside of the immediate catalytic pocket are important for the recognition of structural features surrounding pTyr and the hydrolysis of pTyr-containing peptides/proteins.

In summary, we demonstrate here that the Tyr residue in the KNRY motif (Tyr262 in RPTPα-D1) and the general acid Asp in the WpD motif play an important role to facilitate catalysis through transition-state stabilization. Since all RPTP-D2s lack this Tyr residue, which is located in the pTyr-binding pocket, as well as the general acid/base Asp, it is unlikely that residual PTP activity of RPTP-D2s, if any, has relevance in vivo. Indeed, RPTPα-D1 expressed alone is an active PTP with an activity close to that of full-length RPTPα (*17*, *48*). We show that RPTPα-D2 binds β-naphthyl phosphate, a pTyr analogue, with affinity comparable to that of D1. In addition, substitution of Tyr262 in D1 for Val or Val555 in D2 for Tyr has little effect on binding. These results suggest that RPTP-D2s may be able to bind pTyr-containing proteins. However, whether RPTP-D2s function through binding pTyr-containing proteins, thereby adding a level of specificity and possibly bringing RPTP-D1 and substrate(s) into close proximity, remains to be determined. It is important to point out that, despite their lack of catalytic activity, D2s are highly conserved. In fact, the sequences of different D2s are more closely related to one another than to the D1 in the same PTP (*24*). The overall structure of RPTPα-D2 is highly similar to the structure of other PTPs.[2] Apparently, there is evolutionary conservation of D2s in sequence and structure, suggesting that D2s may play important roles in processes other than catalysis.

NOTE ADDED IN PROOF

Recently, Pallen and co-workers also demonstrated that the KNRY and WpD motifs play an important role in RPTPα-D2 catalytic activity (Lim, K. L., Kolatkar, P. R., Ng, K. P., Ng, C. H., and Pallen, C. J. (1998) *J. Biol. Chem. 273*, 28986−28993).

ACKNOWLEDGMENT

We would like to thank Alex Bilwes and Joe Noel (SBL, the Salk Institute, La Jolla, CA) for providing the coordinates of the RPTPα-D2 crystal structure prior to publication. In addition, we would like to thank Christophe Blanchetot for useful discussions.

REFERENCES

1. Neel, B. G., and Tonks, N. K. (1997) *Curr. Opin. Cell Biol. 9*, 193−204.
2. Fischer, E. H., Charbonneau, H., and Tonks, N. K. (1991) *Science 253*, 401−406.
3. Zhang, Z. Y., Wang, Y., Wu, L., Fauman, E., Stuckey, J. A., Schubert, H. L., Saper, M. A., and Dixon, J. E. (1994) *Biochemistry 33*, 15266−15270.
4. Zhang, Z.-Y. (1997) *Curr. Top. Cell. Regul. 35*, 21−68.
5. Guan, K. L., and Dixon, J. E. (1991) *J. Biol. Chem. 266*, 17026−17030.
6. Pot, D. A., and Dixon, J. E. (1992) *J. Biol. Chem. 267*, 140−142.
7. Barford, D., Flint, A. J., and Tonks, N. K. (1994) *Science 263*, 1397−1404.
8. Stuckey, J. A, Schubert, H. L., Fauman, E. B, Zhang, Z.-Y., Dixon, J. E., and Saper, M. A. (1994) *Nature 370*, 571−575.
9. Bilwes, A. M., den Hertog, J., Hunter, T., and Noel, J. P. (1996) *Nature 382*, 555−559.
10. Hoffmann, K. M., Tonks, N. K., and Barford, D. (1997) *J. Biol. Chem. 272*, 27505−27508.
11. Hof, P., Pluskey, S., Dhe-Paganon, S., Eck, M. J., and Shoelson, E. (1998) *Cell 92*, 441−450.
12. Charbonneau, H., Tonks, N. K., Walsh, K. A., and Fischer, E. H. (1988) *Proc. Natl. Acad. Sci. U.S.A. 85*, 7182−7186.
13. den Hertog, J., Pals, C. E. G. M., Peppelenbosch, M. P., Tertoolen, L. G. J., de Laat, S. W., and Kruijer, W. (1993) *EMBO J. 12*, 3789−3798.
14. Desai, D. M., Sap, J., Silvennoinen, O., Schlessinger, J., and Weiss, A. (1994) *EMBO J. 13*, 4002−4010.
15. Kokel, M., Borland, C. Z., DeLong, L., Horvitz, H. R., and Stern, M. J. (1998) *Genes Dev. 12*, 1425−1437.
16. Wang, Y., and Pallen, C. J. (1991) *EMBO J. 10*, 3231−3237.
17. Wu, L., Buist, A., den Hertog, J., and Zhang, Z.-Y. (1997) *J. Biol. Chem. 272*, 6994−7002.
18. Krueger, N. X., Streuli, M., and Saito, H. (1990) *EMBO J. 9*, 3241−3252.
19. Levy, J. B., Canoll, P. D., Silvenoinen, O., Barnea, G., Morse, B., Honegger, A. M., Huang, J.-T., Cannizzaro, L. A., Park, S.-H., Druck, T., Huebner, K., Sap, J., Ehrlich, M., Musacchio, J. M., and Schlessinger, J. (1993) *J. Biol. Chem. 268*, 10573−10581.
20. Streuli, M., Krueger, N. X., Tsai, A. Y. M., and Saito, H. (1989) *Proc. Natl. Acad. Sci. U.S.A. 86*, 8698−8702.
21. Streuli, M., Krueger, N. X., Thai, T., Tang, M., and Saito, H. (1990) *EMBO J. 9*, 2399−2407.
22. Gebbink, M. F. B. G., Verheijen, M. H. G., van Etten, I., and Moolenaar, W. H. (1993) *Biochemistry 32*, 13512−13522.
23. Itoh, M., Streuli, M., Krueger, N. X., and Saito, H. (1992) *J. Biol. Chem. 267*, 12356−12363.
24. Yang, Q., and Tonks, N. K. (1993) *Adv. Protein Phosphatases 7*, 359−372.
25. Zhang, Z.-Y., Maclean, D., Thieme-Sefler, A. M., Roeske, R., and Dixon, J. E. (1993) *Anal. Biochem. 211*, 7−15.
26. Guan, K. L., and Dixon, J. E. (1991) *Anal. Biochem. 192*, 262−267.
27. Sap, J., D'Eustachio, P., Givol, D., and Schlessinger, J. (1990) *Proc. Natl. Acad. Sci. U.S.A. 87*, 6112−6116.
28. den Hertog, J., Tracy, S., and Hunter, T. (1994) *EMBO J. 13*, 3020−3032.
29. Gordon, J. A. (1991) *Methods Enzymol. 201*, 477−482.
30. Chen, L., Montserat, J., Lawrence, D. S., and Zhang, Z.-Y. (1996) *Biochemistry 35*, 9349−9354.
31. Crans, D. C. (1994) *Comments Inorg. Chem. 16*, 1−33.
32. Brady-Kalnay, S. M., and Tonks, N. K. (1994) *Curr. Opin. Cell Biol. 7*, 6650−6657.
33. Zhang, Z.-Y., Wang, Y., and Dixon, J. E. (1994) *Proc. Natl. Acad. Sci. U.S.A. 91*, 1624−1627.
34. Lohse, D. L., Denu, J. M., Santoro, N., and Dixon, J. E. (1997) *Biochemistry 36*, 4568−4575.
35. Jia, Z., Barford, D., Flint, A. J., and Tonks, N. K. (1995) *Science 268*, 1754−1757.
36. Juszczak, L. J., Zhang, Z.-Y., Wu, L., Gottfried, D. S., and Eads, D. D. (1997) *Biochemistry 36*, 2227−2236.
37. Lu, L., Notkins, A., and Lan, M. (1994) *Biochem. Biophys. Res. Commun. 204*, 930−936.
38. Lan, M., Lu, J., Goto, Y., and Notkins, A. (1994) *DNA Cell Biol. 13*, 505−514.
39. Johnson, P., Ostergaard, H. L., Wasden, C., and Trowbridge, I. S. (1992) *J. Biol. Chem. 267*, 8035−8041.
40. Hengge, A. C., Sowa, G., Wu, L., and Zhang, Z.-Y. (1995) *Biochemistry 34*, 13982−13987.

41. Denu, J. M., Lohse, D. L., Vijayalakshmi, J., Saper, M. A., and Dixon, J. E. (1996) P*roc. Natl. Acad. Sci. U.S.A. 93*, 2493−2498.
42. Pannifer, A. D. B., Flint, A. J., Tonks, N. K., and Barford, D. (1998) *J. Biol. Chem. 273*, 10454−10462.
43. Zhao, Y., and Zhang, Z.-Y. (1996) *Biochemistry 35*, 11797−11804.
44. Sarmiento, M., Zhao, Y., Gordon, S. J., and Zhang, Z.-Y. (1998) *J. Biol. Chem. 273*, 26368−26374.
45. Flint, A. J., Tiganis, T., Barford, D., and Tonks, N. K. (1997) *Proc. Natl. Acad. Sci. U.S.A. 94*, 1680−1685.
46. Alhambra, C., Wu, L., Zhang, Z.-Y., and Gao, J. (1998) *J. Am. Chem. Soc. 120*, 3858−3866.
47. Mildvan, A. S., Weber, D. J., and Kuliopulos, A. (1992) *Arch. Biochem. Biophys. 294*, 327−340.
48. Lim, K. L., Lai, D. S., Kalousek, M. B., Wang, Y., and Pallen, C. J. (1997) *Eur. J. Biochem. 245*, 693−700.
49. Thomas, M. L., Reynolds, P. J., Chain, A., Ben-Neriah, Y., and Trowbridge, I. S. (1987) *Proc. Natl. Acad. Sci. U.S.A. 84*, 5360−5363.
50. Strueli, M., Krueger, N. X., Hall, L. R., Schlossman, S. F., and Saito, H. (1988) *J. Exp. Med. 168*, 1553−1562.
51. Gebbink, M. F. B. G., van Etten, I., Hateboer, G., Suijkerbuijk, R., Beijersbergen, R., van Kessel, A. G., and Moolenaar, W. H. (1991) *FEBS Lett. 290*, 123−130.
52. Chernoff, J., Schievella, A. R., Jost, C. A., Erikson, R. L., and Neel, B. G. (1990) *Proc. Natl. Acad. Sci. U.S.A. 87*, 2735−2739.
53. Cool, D. E., Tonk, N. K., Charbonneau, H., Walsh, K. A., Fischer, E. H., and Krebs, E. G. (1989) *Proc. Natl. Acad. Sci. U.S.A. 86*, 5257−5261.
54. Yang, Q., Co, D., Sommercorn, J., and Tonks, N. K. (1993) *J. Biol. Chem. 268*, 6622−6628.
55. Shen, S. H., Bastien, L., Posner, B. I., and Chretien, P. (1991) *Nature 352*, 736−739.
56. Gu, M., Warshawsky, I., and Majerus, P. W. (1992) *Proc. Natl. Acad. Sci. U.S.A. 89*, 2980−2984.

BI981936B